#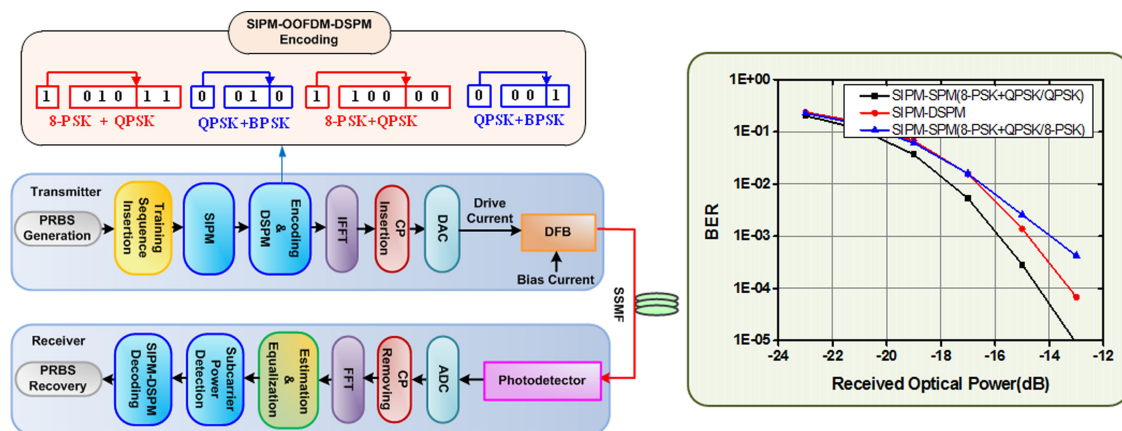 Subcarrier Index-Power Modulated-Optical OFDM With Dual Superposition Multiplexing for Directly Modulated DFB-Based IMDD PON Systems

Lin Chen
Fadi Halabi
Roger Philip Giddings
Junjie Zhang
Jianming Tang

Subcarrier Index-Power Modulated-Optical OFDM With Dual Superposition Multiplexing for Directly Modulated DFB-Based IMDD PON Systems

Lin Chen [ORCID],[1] **Fadi Halabi** [ORCID],[2] **Roger Philip Giddings** [ORCID],[2]
Junjie Zhang [ORCID],[3] **and Jianming Tang** [ORCID] [2]

[1]College of Electronics and Information Engineering, Shanghai University of Electric Power, Shanghai 200090, China
[2]School of Electronic Engineering, Bangor University, Bangor LL57 1UT, U. K.
[3]Key Laboratory of Specialty Fiber Optics and Optical Access Networks, Joint International Research Laboratory of Specialty Fiber Optics and Advanced Communication, Shanghai Institute for Advanced Communication and Data Science, Shanghai University, Shanghai 200444, China

Abstract: A low-signal-modulation format-enabled highly spectrally efficient new transmission technique termed subcarrier index-power modulated optical OFDM with dual superposition multiplexing (SIPM-OOFDM-DSPM) is proposed and investigated, for the first time, in intensity modulation and direct detection (IMDD) passive optical network (PON) systems incorporating directly modulated DFB lasers (DMLs). The DSPM operation passively adds two low-signal-modulation format-encoded complex numbers and assigns the sum to subcarrier index-power modulation (SIPM)-generated low- and high-power subcarriers. Detailed numerical explorations of SIPM-OOFDM-DSPM performances over additive white Gaussian noise channels are undertaken, based on which optimum key transceiver parameters are identified. In comparison with previously published techniques, over simple DML-based IMDD PON systems, SIPM-OOFDM-DSPM considerably improves the signal transmission capacity, system power budget, and performance tolerance to both chromatic dispersion and fiber nonlinearity. The work suggests that SIPM-OOFDM-DSPM is a promising signal transmission technique capable of providing cost-sensitive PON systems with improved transmission capacity, performance flexibility, and adaptability.

Index Terms: Direct modulated DFB lasers and passive optical networks, digital signal processing, orthogonal frequency division multiplexing, signal modulation.

1. Introduction

The fifth generation (5G) of mobile networks offer immense transmission bandwidths, support massive machine-type communications, and deliver low-latency and ultra-reliable real-time services [1].

To practically implement 5G networks, huge technical challenges have to be addressed across all layers. To establish a physical-layer communication connection capable of delivering the targeted high signal transmission capacity, for cost-sensitive application scenarios, the utilization of low-cost and low-bandwidth optical/electrical devices is greatly advantageous, which unavoidably require sophisticated multiplexing techniques to achieve highly spectrally efficient signal transmissions. A number of signal multiplexing solutions have been reported including massive multiple-input/multiple-output (MIMO) [2] and non-orthogonal multiple access (NOMA) [3]. Conventional MIMO can achieve high spectral efficiency with massive antennas, but it suffers the low energy utilization efficiency due to radio frequency (RF) chain-induced extra power consumption. On the other hand, NOMA employs successive interference cancellation to improve the signal spectral efficiency, which, however, results in additional digital signal processing (DSP) complexity in the receiver and a relatively large latency. Given the fact that spectrally efficient orthogonal frequency division multiplexing (OFDM) has already been adopted in 4G mobile networks, the combination of OFDM with a suitable signal multiplexing technique is a promising solution for cost-sensitive 5G systems [4].

Recently considerable interest has been focused on further improving the spectral efficiency of the traditional OFDM technique. In 2009, subcarrier-index modulated OFDM (SIM-OFDM) [5] was reported, in which the subcarrier index is employed as an extra information-carrying dimension. Inspired by the underlying idea of SIM, the concept of OFDM with index modulation (OFDM-IM) was also reported [6], in which a maximum likelihood (ML) detector is used in the receiver to detect active subcarriers within each individual OFDM symbol. For a large subcarrier count, the ML-associated DSP complexity grows exponentially. OFDM-IM was further modified and its performance was analyzed for different applications [7], [8]. More importantly, in comparison with conventional OFDM, the achievable signal transmission capacities and spectral efficiencies of both SIM-OFDM and OFDM-IM are almost halved since only half of the subcarriers are activated for data transmission.

To address the aforementioned challenges associated with SIM-OFDM and OFDM-IM, subcarrier index-power modulated optical OFDM (SIPM-OOFDM) has been published and its application in intensity modulation and direct detection (IMDD) passive optical network (PON) systems have been explored [9], [10]. In SIPM-OOFDM, subcarrier index and subcarrier power are jointly utilized to create an energy-free extra information-carrying dimension to convey additional information bits. In generating a SIPM-OOFDM signal, a high (low) power is assigned to a subcarrier according to an incoming pseudo random bit sequence (PRBS) stream, and the subcarrier is then encoded using 8-phase shift keying (8-PSK) (quadrature phase shift keying (QPSK)). As a direct result of such an encoding operation, all of the subcarriers are always activated, thus leading to a 17% increase in signal transmission capacity and an 0.9 dB reduction in minimum required signal-to-noise ratio (SNR) corresponding to a bit error rate (BER) of 1.0×10^{-3}, in comparison with conventional OFDM encoded using 8-QAM [10]. A further increase in signal transmission capacity is also achievable when superposition multiplexing (SPM) is introduced into SIPM-OOFDM, here referred to as (SIPM-OOFDM-SPM) [11]. In SIPM-OOFDM-SPM, high power subcarriers use SPM to passively add two complex numbers encoded by 8-PSK and QPSK, with all of the low power subcarriers still employing QPSK only. In comparison with SIPM-OOFDM, SIPM-OOFDM-SPM improves the power utilization efficiency of high power subcarriers, thus resulting in a further increase in signal transmission capacity. Based on both SIPM-OOFDM and SIPM-OOFDM-SPM, a very interesting open question can be raised, as to whether SPM can also be employed in both low and high power subcarriers to further improve the signal power usage efficiency and signal transmission capacity.

To address the open question concerning its use in IMDD PON transmission systems incorporating directly modulated DFB lasers (DMLs), an improved variant of SIPM-OOFDM-SPM known as SIPM-OOFDM with dual superposition multiplexing (SIPM-OOFDM-DSPM) is proposed, for the first time, in this paper. In SIPM-OOFDM-DSPM, the addition SPM operation of two 8-PSK- and QPSK-encoded complex numbers is applied for high power subcarriers, whilst for low power subcarriers, two QPSK- and BPSK-encoded complex numbers are also passively added, and the resulting sum is assigned to the corresponding subcarrier. As such SIPM-OOFDM-DSPM enables

a more effective use of both low and high power subcarriers without significantly increasing the DSP complexity.

For the considered IMDD PON systems, the proposed SIPM-OOFDM-DSPM technique enables an increase of approximately 11.1% in signal transmission capacity compared to the previously published (8-PSK + QPSK)/QPSK-encoded SIPM-OOFDM-SPM. In addition, in comparison with (8-PSK + QPSK)/8-PSK-encoded SIPM-OOFDM-SPM capable of supporting the same signal transmission capacity, SIPM-OOFDM-DSPM improves the system power budget and performance tolerances against both chromatic dispersion and fiber nonlinearity for IMDD PON systems incorporating ideal intensity modulators or DMLs.

The paper is organized as following: in Section 2, the SIPM-OOFDM-DSPM operating principle is described and the corresponding transceiver architecture is presented with special attention given to information encoding and decoding procedures and subcarrier power threshold determinations. In Section 3, a set of optimum key transceiver parameters are numerically identified, based on which the achievable SIPM-OOFDM-DSPM transmission performance can be maximized. In Section 4, by making use of the optimum transceiver parameters, extensive explorations of achievable SIPM-OOFDM-DSPM transmission performances are undertaken in terms of signal transmission capacity, chromatic dispersion tolerance and Kerr effect-related fiber nonlinearity tolerance over IMDD PON system incorporating ideal intensity modulators. In addition, SIPM-OFDM-DSPM transmission performances are also investigated over DML-based IMDD PON systems. Finally, the paper is summarized in Section 5.

2. SIPM-OOFDM-DSPM Operating Principle and Transceiver Design

The SIPM-OOFDM-DSPM transceiver DSP and hardware architectures are very similar to SIPM-OOFDM-SPM [11]. The major difference between them is that the mapping/de-mapping procedure is altered in SIPM-OOFDM-DSPM, as detailed below: in the transmitter, a SIPM operation-produced low power subcarrier is allocated with the sum of QPSK- and BPSK-encoded complex values, and a SIPM operation-produced high power subcarrier is still allocated with the sum of 8-PSK- and QPSK-encoded complex values. For instance, for an incoming PRBS stream, if a "0" ("1") bit arrives, the SIPM operation is firstly applied to assign the subcarrier at a low (high) power level. After that, the following 3 (5) bits of the same PRBS stream are truncated, the first 2 (3) bits of which are encoded with QPSK (8-PSK) and the remaining 1 (2) bits are encoded with BPSK (QPSK). Having completed the above operations, a passive summation of these two QPSK- and BPSK-encoded (8-PSK- and QPSK-encoded) complex numbers is conducted and the sum is subsequently assigned to the corresponding subcarrier at the low (high) power level, as seen in Fig. 1(a) and (b). It is easy to see that such a summation operation for the low and high power subcarriers allows each low (high) power subcarrier to convey 4 (6) information bits in total. To gain a better understanding of the abovementioned encoding operation, the constellations of the proposed technique are illustrated in Fig. 1(c), where two (four) information-conveying satellite constellation points surround each virtual QPSK (8-PSK) constellation point occurring in the low (high) power subcarriers encoded using QPSK (8-PSK) and BPSK (QPSK). It can be seen in Fig. 1(c) that there are 8 (32) information-conveying satellite constellation points for a low (high) power subcarrier, suggesting that (8-PSK + QPSK)/(QPSK + BPSK)-encoded SIPM-OOFDM-DSPM delivers a signal bit rate equal to (8-PSK + QPSK)/8-PSK-encoded SIPM-OOFDM-SPM.

In the receiver, after the fast Fourier transform (FFT) and standard training sequence-based channel estimation and equalization, a threshold decision DSP function is introduced to differentiate between the received high and low power subcarriers. The subcarrier power threshold, $P_{\text{threshold}}$, is defined as:

$$P_{\text{threshold}} = \frac{\min\left(P_{8-PSK+QPSK}\right) + \max\left(P_{QPSK+BPSK}\right)}{2} \qquad (1)$$

where $P_{8-PSK+QPSK}$ and $P_{QPSK+BPSK}$ are the received high and low subcarrier powers respectively. As a direct consequence of the DSPM operation, $P_{8-PSK+QPSK}$ and $P_{QPSK+BPSK}$ varies slightly from
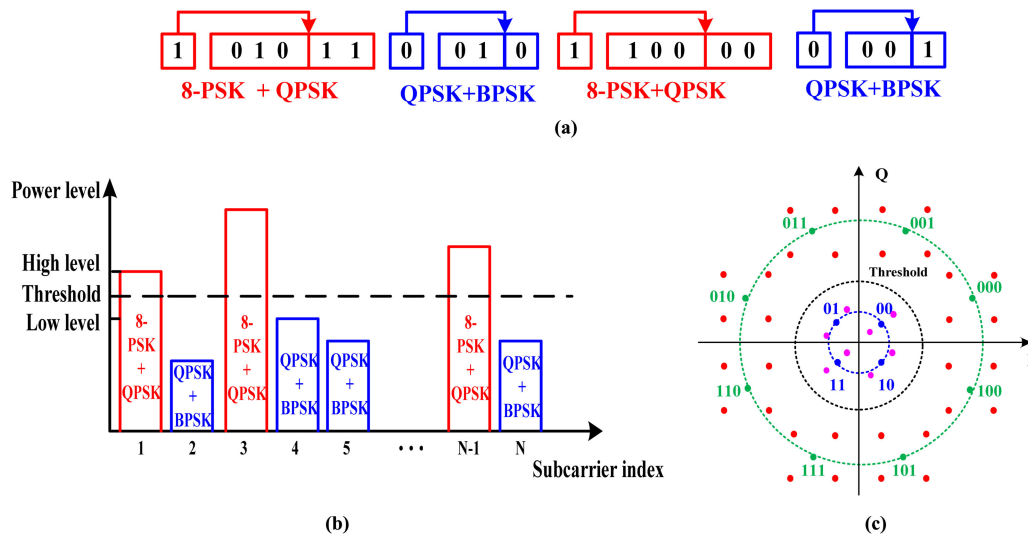
Fig. 1. (a) SIPM-OOFDM-DSPM data encoding process in the transmitter, (b) A schematic diagram showing how subcarriers of different power levels in the transmitter are assigned, and (c) overall SIPM-OOFDM-DSPM constellations.

subcarrier (symbol) to subcarrier (symbol), as illustrated in Fig. 1(c). Therefore the minimum value of $P_{8-PSK+QPSK}$ and the maximum value of $P_{QPSK+BPSK}$ are used in Eq. (1) to effectively differentiate between $P_{8-PSK+QPSK}$ and $P_{QPSK+BPSK}$. The obtained subcarrier power threshold is subcarrier index-dependent and is averaged periodically. The averaged threshold is then employed to recover the information bit carried in the subcarrier index-power dimension, i.e., a "0" ("1") information bit is recovered when the detected subcarrier power level is below (above) the subcarrier power threshold. Once the subcarrier power level decision is made, the corresponding information bits carried by the subcarrier in the conventional subcarrier-information-carrying dimension can be recovered using the SIPM-OOFDM-SPM approach presented in [11]: after equalization, for low and high power subcarriers, 8 (32) comparisons between the received complex value and all possible "to be recovered" ideal complex values are made, the combination that results in the smallest difference is used to recover the information carried by the subcarrier. SIPM-OOFDM-DSPM increases the de-mapping DSP complexity by a factor of approximately 3 in comparison with conventional 32-QAM-encoded OOFDM. This is similar to SIPM-OOFDM-SPM. However, as indicated in [11], the FPGA logic resource consumed by the de-mapping function is almost negligible compared to the total FPGA logic resource consumed by all other DSP functions embedded in the transmitter or receiver. Finally, the error propagation removal approach reported in SIPM-OOFDM [10] and SIPM-OOFDM-SPM [11] is also applicable in the proposed technique.

The main attributes associated with the proposed signal modulation technique are: (1) The low signal modulation formats enable high signal transmission capacities while preventing a considerable increase in transceiver DSP and hardware complexity; (2) Transceiver design flexibility is improved, since both hardware and DSP resources remain almost the same for SIPM-OOFDM, SIPM-OOFDM-SPM and SIPM-OOFDM-DSPM; (3) Performance adaptability is enhanced, as the transmission performance characteristics are dynamically variable by only altering DSP design according to the requirements of different application scenarios.

A schematic diagram illustrating the SIPM-OOFDM-DSPM transmission link is shown in Fig. 2, where a standard single-mode fibre (SSMF) connecting the transmitter and the receiver is employed. In the transmitter, a training sequence is periodically inserted into the data sequence. After the SIPM operation, the DSPM operation is undertaken using BPSK, QPSK and 8-PSK signal modulation formats. The main DSP functions incorporated in the SIPM-OOFDM-DSPM transmitter include: serial to parallel (S/P) conversion, inverse fast Fourier transform (IFFT), cyclic prefix addition,
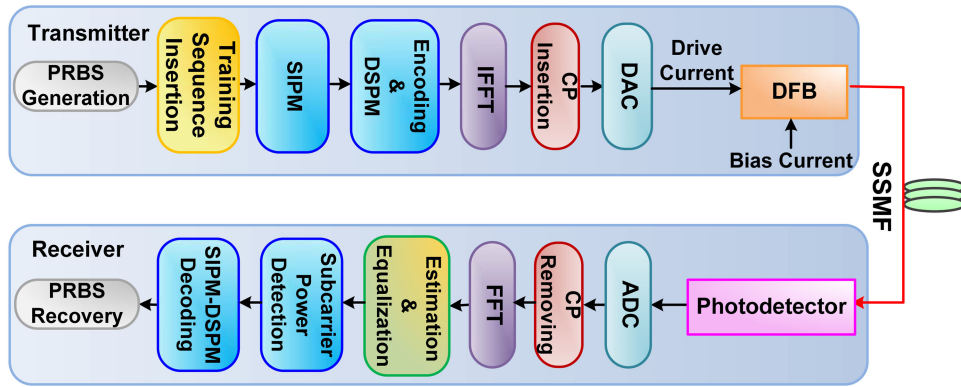
Fig. 2. Representative SIPM-OOFDM-DSPM transceiver architecture in a DML-based IMDD PON system.

parallel to serial (P/S) conversion, and digital to analog converter (DAC). Prior to the IFFT, the subcarriers and their conjugate counterparts are arranged to satisfy the Hermitian symmetry in order to obtain a real-valued electric OFDM signal. Finally, the combination of the electric OFDM signal and an optimum DC current is conducted, the combined current directly drives a 1550 nm DML to generate an optical OFDM (OOFDM) signal. The generated optical signal is then launched into the considered IMDD PON link.

An SSMF simulation model based on the split-step Fourier procedure is used to simulate the optical signal propagation over the IMDD PON system. In the model, the impacts of fiber loss, chromatic dispersion and Kerr effect-related fibre nonlinearities are included [12].

After the fiber transmission, a square-law photodetector subject to both shot and thermal noise is employed in the receiver. As described in Fig. 2, to recover data from the low-pass-filtered electrical signal, major DSP functions are used, which include cyclic prefix deletion, FFT, channel estimation and equalization, subcarrier power detection, subcarrier power threshold calculation, recovery of information bits in both the subcarrier index-power dimension and the conventional subcarrier-information-carrying dimension.

3. Optimisation of Key Transceiver Parameters

Having described the SIPM-OOFDM-DSPM transceiver design principle in Section 2, optimum key transceiver parameters that can maximize the achievable transmission performance of the technique are identified in this section. To explicitly highlight the benefits associated with the proposed technique, performance comparisons are made between SIPM-OOFDM-DSPM, (8-PSK + QPSK)/QPSK-encoded SIPM-OOFDM-SPM and (8-PSK + QPSK)/ 8-PSK-encoded SIPM-OOFDM-SPM for all considered cases discussed in the following sections.

By using the default parameters listed in Table 1, the optimum SIPM-OOFDM-DSPM signal clipping ratio of 12 dB and the optimum 9 quantization bits of the corresponding DAC/ADC are identified, which are identical to those corresponding to SIPM-OOFDM-SPM [11]. In Table 1, a cyclic prefix (CP) of 25% is chosen to enable fair performance comparisons with previously published results where identical CPs are adopted [9]–[11]. In practice, for a specific transmission system, there exists an optimum CP, which gives rise to a maximized net signal bit rate and still maintains the system performance stability and robustness at an acceptable level. Unless explicitly mentioned, these parameters are utilized as default parameters in Section 3 and Section 4 of the paper. To improve the subcarrier power utilization efficiency, particular attention is given here to the following four parameters: a) the power ratio between the high and low power subcarriers; b) initial phase setting in the low power subcarriers; c) the relationship between initial phase of the low and high power subcarriers, and d) the phase rotation of the BPSK constellation points.

TABLE 1

Transceiver and Transmission System Parameters

Parameter	Value
Total number of IFFT/FFT points	64
Data-carrying subcarriers	31
Modulation formats	Low power subcarriers: BPSK +QPSK
	High power subcarriers: 8-PSK +QPSK
PRBS stream	500,000 bits
Cyclic prefix	25%
Modulator and PIN bandwidths	12.5 GHz
DAC & ADC sampling rate	12.5 GS/s
DAC & ADC bit resolution	9 bits
DAC & ADC clipping ratio	12 dB
Power ratio between BPSK and QPSK	0.4
Power ratio between QPSK and 8-PSK	3.25
Initial phase setting	Low power subcarriers: 45º
	High power subcarriers:34º
PIN responsivity	0.8 A/W
PIN detector sensitivity	-19 dBm*
Linear fiber attenuation	0.2 dB/km
SSMF dispersion slope at 1550 nm	0.07 ps/nm/nm/km
SSMF dispersion parameter at 1550 nm	16 ps/(nm.km)
Kerr coefficient	2.35×10^{-20} m²/W
Effective area	80μm²

*Corresponding to 10 Gb/s non-return-to-zero data at a BER of 1.0×10^{-9}

As SIPM-OOFDM-DSPM has two different subcarrier power levels, to evenly distribute the constellation points over the whole constellation space corresponding to a given signal power, it is easy to understand that the optimization of subcarrier power level plays an important role in determining the performance of the technique. The power ratio of low (high) power subcarriers, PR_L (PR_H) is defined as

$$PR_L = \frac{P_{BPSK}}{P_{QPSK}}, \quad PR_H = \frac{P_{8-PSK}}{P_{QPSK}} \tag{2}$$

where P_{BPSK}, P_{QPSK} and P_{8-PSK} denote the signal powers encoded using BPSK, QPSK and 8-PSK respectively. In order to identify the optimum power ratio values, Fig. 3(a) explores the power ratio-dependent BER performance over additive white Gaussian noise (AWGN) channels at a SNR of 24 dB. As presented in Fig. 3(a), the optimum power ratio of low (high) power subcarriers, PR_L (PR_H), is 0.4 (3.25). For a PR_L less than 0.4, the BER rises considerably due to the rapid decrease in the minimum Euclidean distance between the SPM-generated 8 constellation points taken by the low power subcarriers, whilst for a PR_L greater than 0.4, the BER also grows sharply due to the rapid reduction in the power difference between high and low subcarrier powers. Similar to the low power subcarrier case, an optimum power ratio of 3.25 for high power subcarriers is also identified in the same figure, which occurs due to the similar mechanism explained above.

Apart from the optimum subcarrier power ratio, as shown in Fig. 1(c), the minimum Euclidean distance between SPM-generated 8 (32) constellation points taken by the low (high) power subcarriers can also be maximized by a phase rotation of BPSK (QPSK) with respect to QPSK (8-PSK). The effectiveness of such phase rotation operation is demonstrated in Fig. 3(b), where BER performances versus initial QPSK phase setting are plotted over AWGN channels at a SNR of 24 dB for SIPM-OOFDM-DSPM. The BER curve has a periodically varying pattern. Fig. 3(b) indicates that with respect to BPSK, an optimum initial QPSK phase setting is 45° for DSPM, which is due to the maximized minimum Euclidean distance for the low power subcarriers. An optimum difference of 90° between the two successive optimum QPSK phase settings is also shown in the figure. It should be noted that compared to SIPM-OOFDM-SPM, the similar encoding operation is employed in the high power subcarriers, the optimum 34° QPSK initial phase setting with respect to 8-PSK,
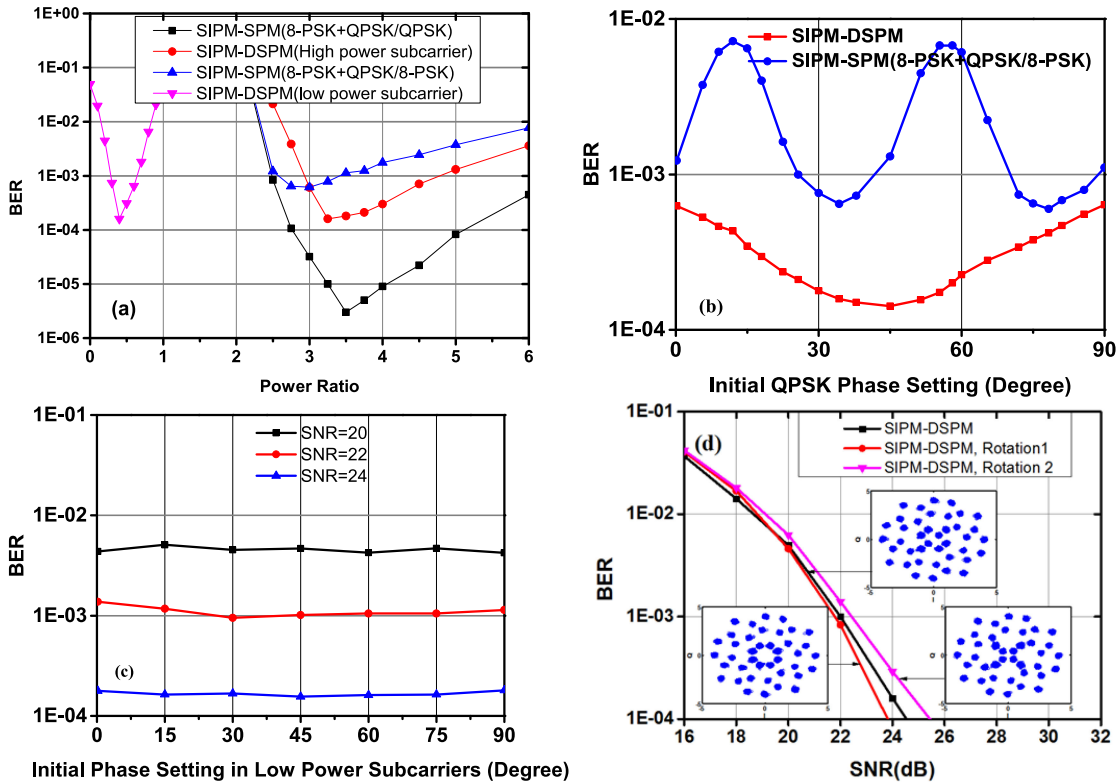
Fig. 3. Optimization of transceiver parameters. (a) BER versus power ratio, (b) Optimum initial QPSK phase setting, (c) BER versus initial phase setting in low power subcarriers, (d) ±90° phase rotation of the BPSK constellation points. Here AWGN channels are considered in all simulations.

as reported in [11], is thus still applicable in SIPM-OOFDM-DSPM for the high power subcarriers, as seen in Fig. 3(b).

In order to have an in-depth understanding of the aforementioned optimization processes, the relationship of initial phase setting for the low and high power subcarriers are presented in Fig. 3(c). In simulating Fig. 3(c), different SNR values are considered and the initial phase in the high power subcarrier is fixed at 34°. As shown in Fig. 3(c), the BER curves for the initial phase in the low power subcarriers remain almost constant. It is also shown that the optimum initial phase setting for the low power subcarrier is not affected by the high power subcarrier. This implies that the DSPM operation can provide a simple and effective approach for independently manipulating the signal constellation in order to satisfy the requirement of a specific application without impacting the overall signal performance.

To further maximize the minimum Euclidian distance for the low power subcarriers, with respect to QPSK, a phase rotation of ±90° should also be applied to the BPSK constellation points. Fig. 3(d) shows BER versus SNR performances for such a phase rotation operation over AWGN channels. In order to explicitly demonstrate the impact of the phase rotation on the BER versus SNR performance, the equalized overall SIPM-OOFDM-DSPM constellations for the cases of including and excluding the rotated BPSK phase are also presented in Fig. 3(d). In numerically simulating Fig. 3(d), all the default parameters given in Table 1 are used. As illustrated in Fig. 3(d), SIPM-DSPM Rotation 1 denotes that the BPSK constellation points are rotated by ±90° with respect to QPSK constellation points, which are superposed with either '00' or '11'; On the other hand, SIPM-DSPM Rotation 2 denotes that the BPSK constellation points are rotated by ±90° with respect to QPSK constellation points, which are superposed with either '01' or '10'. Interestingly, by comparing these three BER curves for SIPM-DSPM, SIPM-DSPM Rotation 1 and SIPM-DSPM Rotation 2, it is noted

TABLE 2

Signal BIT RATE Comparisons

Modulation Formats	Signal Bit Rate (Gb/s)
(8-PSK+QPSK)/QPSK-encoded SIPM-OOFDM-SPM	26.71
(8-PSK+QPSK)/(QPSK+BPSK)-encoded SIPM-OOFDM-DSPM	29.67
(8-PSK+QPSK)/8-PSK-encoded SIPM-OOFDM-SPM	29.67

that the Rotation 1 operation gives rise to an almost 0.2 dB SNR gain at a BER of 1.0×10^{-3}. The physical reason behind the observed SNR gain is an increase between the minimum value of $P_{8-PSK+QPSK}$ and the maximum value of $P_{QPSK+BPSK}$, as shown in the corresponding constellation diagrams inserted in Fig. 3(d). Such an increased difference between the low and high subcarrier power levels considerably eases the subcarrier power level detection, thus leading to a reduction in the error propagation effect. As such in the remaining parts of the paper, the $\pm 90°$ phase Rotation 1 operation is adopted in simulating the SIPM-OOFDM-DSPM transmission performances for all the considered cases.

4. SIPM-OOFDM-DSPM Transmission Performance

Based on the optimum transceiver parameters obtained in Section 3, in this section, the maximum achievable transmission performance of SIPM-OOFDM-DSPM is explored over AWGN and different IMDD PON systems.

To simulate the performance of the SIPM-OOFDM-DSPM technique over IMDD PON systems, the following conditions are used: a PIN photodetector with a responsivity of 0.8 A/W and a receiver sensitivity of -19 dBm (corresponding to a 10 Gb/s non-return-to-zero at a BER of 1.0×10^{-9}), and an SSMF with a chromatic dispersion parameter of 16.0 ps/(km·nm), a dispersion slope of 0.07 ps/nm/nm/km, a linear fiber loss of 0.2 dB/km, an effective area of 80 μm^2 and a Kerr coefficient of 2.35×10^{-20} m^2/W. All other parameters that are not explicitly specified above are stated in the corresponding texts when necessary.

4.1 Signal Bit Rate Performance

The SIPM-OOFDM-DSPM signal transmission capacity, R_b, is calculated using the following formula:

$$R_b = \frac{f_S \left[\rho_H \left(b_H + 1 \right) + \rho_L \left(b_L + 1 \right) \right] \left(N - 2 \right)}{2N \left(1 + \alpha \right)} \tag{3}$$

where ρ_L (ρ_H) is the occurrence probability of BPSK + QPSK (8-PSK + QPSK)-encoded low (high) power subcarriers and b_L (b_H) is the number of binary information bits conveyed by each low (high) power subcarrier within a symbol period; N denotes the total number of subcarrier; f_S denotes the sampling rate of the DAC/ADC, and α is the coefficient representing the signal bit rate reduction induced by the training sequence.

By using the identified optimum transceiver parameters, and by considering 64 subcarriers per symbol, the signal bit rates of the three considered transmission techniques can be easily computed, which are presented in Table 2. It can be seen in Table 2 that SIPM-OOFDM-DSPM has a maximum signal bit rate of 29.67 Gb/s, which outperforms (8-PSK + QPSK)/QPSK-encoded SIPM-OOFDM-SPM by 11.1%. Table 2 also indicates that SIPM-OOFDM-DSPM can provide the same signal bit rate of 29.67 Gb/s, compared to (8-PSK + QPSK)/8PSK-encoded SIPM-OOFDM-SPM where higher signal modulation formats are taken in low power subcarriers. As a direct result, in comparison with (8-PSK + QPSK)/8PSK-encoded SIPM-OOFDM-SPM, the SIPM-OOFDM-DSPM technique gives rise to a reduced minimum received optical power and improved performance tolerance to both chromatic dispersion and fiber nonlinearity, as discussed in the following subsections.
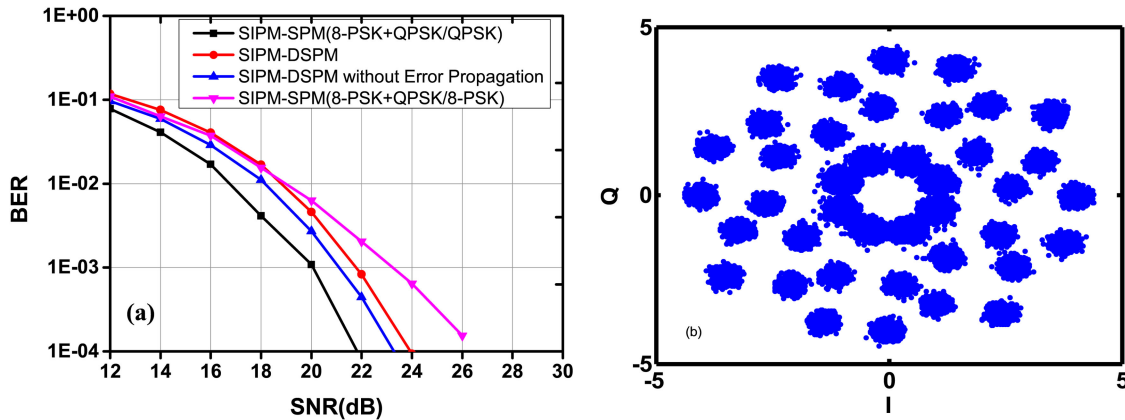
Fig. 4. (a). Overall channel BER performance versus signal SNR over AWGN channels. An error propagation-free SIPM-OOFDM-DSPM BER curve is included. (b) Overall SIPM-OOFDM-DSPM constellation diagram after FFT and equalization in the receiver.

4.2 BER Performance Over AWGN Channels

The BER versus SNR performance of these three considered transmission techniques over AWGN channels is shown in Fig. 4(a), from which it is observed that the 29.67 Gb/s SIPM-OOFDM-DSPM signal results in a SNR gain of approximately 1.8 dB at a BER of 1.0×10^{-3} compared to the 29.67 Gb/s (8-PSK + QPSK)/8PSK-encoded SIPM-OOFDM-SPM signal, whereas the 29.67 Gb/s SIPM-OOFDM-DSPM signal introduces a SNR penalty of approximately 1.9 dB at a BER of 1.0×10^{-3} compared to the 26.71 Gb/s (8-PSK + QPSK)/QPSK-encoded SIPM-OOFDM-SPM signal. The physical mechanism behind the SNR gain is mainly due to the DSPM operation-enhanced minimum Euclidean distance, which reduces the minimum required SNR for a specific BER. Under the identified optimum operating conditions, our simulations show that in comparison with the (8-PSK + QPSK)/8PSK-encoded SIPM-OOFDM-SPM signal, the DSPM operation can increase the minimum Euclidean distance by 4.52% for the low power subcarriers of the SIPM-OOFDM-DSPM signal.

In addition, the SIPM-OOFDM-DSPM BER curve without considering the error propagation effect is plotted in Fig. 4(a). This figure shows that the error propagation removal approach introduces an SNR gain of almost 0.8 dB at a BER of 1.0×10^{-3}. For fair performance comparisons, in the remaining parts of the paper error propagation removal is excluded for both SIPM-OOFDM-DSPM and SIPM-OOFDM-SPM. Finally, an equalised overall SIPM-OOFDM-DSPM constellation diagram at an SNR of 24 dB is shown in Fig. 4(b), where the sizes of the inner constellation points are relatively larger than the outer constellation points. This is because the inner (outer) constellation points are associated with low (high) signal modulation formats. Assuming that each signal modulation format is encoded at an equal probability, thus the occurrence probability of a specific constellation point of the low signal modulation format is higher than that corresponding to the high signal modulation format.

4.3 SIPM-OOFDM-DSPM Transmission Performance Over 25 km IMDD PON Systems

Over 25 km SSMF IMDD PON systems, the BER performance as a function of received optical power for the SIPM-OOFDM-DSPM and SIPM-OOFDM-SPM techniques are presented in Fig. 5(a). In all the three cases considered, an ideal optical intensity modulator is utilized, which produces an optical field signal $S_o(t)$ having a waveform governed by $S_o(t) = \sqrt{y(t)}$, here $y(t) > 0$ is the electrical driving current of the signal with an optimum DC bias current being added. The optical launch power is fixed at 5 dBm. As expected from Fig. 4(a), Fig. 5(a) indicates that SIPM-OOFDM-DSPM can support 29.67 GB/s signal transmission over 25 km SSMF in the considered IMDD PON systems.
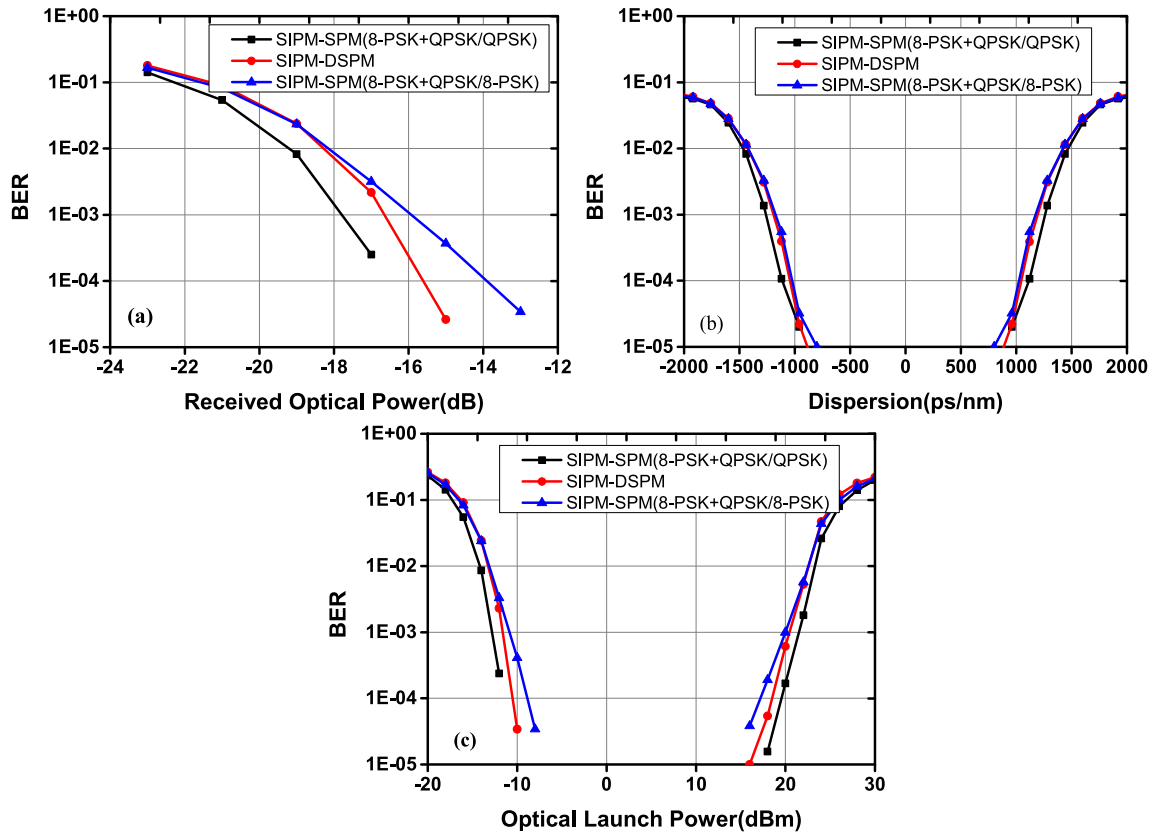
Fig. 5. Transmission performance of the 26.71 Gb/s (8-PSK + QPSK)/QPSK-encoded SIPM-OOFDM-SPM signal, the 29.67 Gb/s SIPM-OOFDM-DSPM signal and the 29.67 Gb/s (8-PSK + QPSK)/8-PSK-encoded SIPM-OOFDM-SPM signal. (a) BERs against received optical power after 25 km SSMF IMDD PON systems transmission. (b) SIPM-OOFDM-DSPM chromatic dispersion tolerance. (c) SIPM-OOFDM-DSPM fibre nonlinearity tolerance.

As shown in Fig. 5(a), the BER performance comparisons between the 29.67 Gb/s SIPM-OOFDM-DSPM signal, the 26.71 Gb/s (8-PSK + QPSK)/QPSK-encoded SIPM-OOFDM-SPM signal and the 29.67 Gb/s (8-PSK + QPSK)/8-PSK-encoded SIPM-OOFDM-SPM signal, show a 1 dB received optical power penalty and a 0.9 dB received optical power gain respectively at a BER of 1.0×10^{-3}. Such an optical power penalty agrees with the electrical SNR penalty observed in Fig. 4(a). It is also indicated that when the single SPM operation is employed, to reach the same signal bit rate, a high-order signal modulation format such as 8-PSK has to be applied, which, however, results in an almost 0.9 dB optical power penalty at a BER of 1.0×10^{-3}, as shown in Fig. 5(a). In summary, the DSPM-induced 11.1% increase in signal transmission capacity causes a 1 dB change to the system power budget at the adopted FEC limit.

At a specific BER, the reduction in received optical power means an improvement in system optical power budget, this results in an improved SIPM-OOFDM-DSPM performance tolerance to both chromatic dispersion and fiber nonlinearity for the considered IMDD PON systems. Such a statement is verified in Fig. 5(b) and Fig. 5(c). For the SIPM-OOFDM-DSPM and SIPM-OOFDM-SPM techniques, the BER against chromatic dispersion is explored in Fig. 5(b). In simulating Fig. 5(b), the fiber dispersion parameters of 16.0 ps/(km·nm) and −16.0 ps/(km·nm) are adopted for the positive and negative chromatic dispersion regions respectively, and the fiber Kerr nonlinearity and linear attenuation are excluded. The transmission distance varies from 10 km to 125 km. As expected, it is shown in Fig. 5(b) that, compared to the 29.67 Gb/s (8-PSK + QPSK)/8-PSK SIPM-OOFDM-SPM signal, the SIPM-OOFDM-DSPM signal with the same signal bit rate widens

TABLE 3
DML Parameters

Parameter	Value
Cavity length	300μm
Cavity thickness	0.033μm
Cavity width	2μm
Photo lifetime	3.6ps
Nonlinear gain coefficient	7.4×10^{-23} m^3
A linewidth enhancement factor	2.1
Rate of refractive index change with carrier density	-1.38×10^{-26} m^{-3}
Transparency carrier density	1.5×10^{24} m^{-3}
Linear gain coefficient	7.5×10^{-20} m^2
Bimolecular recombination coefficient	1.0×10^{-16} m^3/s
Auger recombination coefficient	6.5×10^{-41} m^6/s
Fraction of spontaneous emission	1.0×10^{-5}
Mode confinement factor	0.07
Linear carrier recombination lifetime	1.0×10^{-9}
Optical vertical width	0.47μm
Optical horizontal width	1.80μm
Group refractive index	3.7
Phase refractive index	3.2203
Coupling efficiency from the laser chip to the SMF	0.38

the chromatic dispersion tolerance range by approximately 70 ps/nm at a BER of 1.0×10^{-3}. This arises due to the DSPM operation-induced increase in minimum Euclidean distance for the low power subcarriers, as discussed in Section 4.2.

Apart from the abovementioned enhancement in chromatic dispersion tolerance range, the increase in minimum Euclidean distance also gives rise to an improved optical launch power dynamic range, as shown in Fig. 5(c). The fiber nonlinearity impact on the performances of the three considered transmission techniques are investigated in Fig. 5(c), where the BERs are plotted against optical launch power. In simulating Fig. 5(c), the fiber linear and Kerr nonlinear effects are present, and the transmission distance is fixed at 25 km. It is seen in Fig. 5(c) that, in comparison with (8-PSK + QPSK)/8-PSK-encoded SIPM-OOFDM-SPM, the DSPM operation improves the optical launch power dynamic range by almost 1.5 dB at a BER of 1.0×10^{-3}.

4.4 SIPM-OOFDM-DSPM Transmission Performance in DML-Based IMDD PON Systems

Having discussed the SIPM-OOFDM-DSPM transmission performance in ideal optical intensity modulator-based IMDD PON systems, in this section a lumped DML model [13] is adopted, which takes into account the longitudinal mode spatial hole-burning, linear and nonlinear carrier recombination and nonlinear gain effects. The lumped model is a simplified version of a comprehensive theoretical DFB model [14], and agrees very well with experimental measurements [13], [15]. To numerically simulate the DML at 1550 nm, all the parameter values similar to those reported in [13] are adopted, which are listed in Table 3.

Based on the previously discussed transceiver architecture and its corresponding optimum simulation parameters, investigations are undertaken to identify the optimum DML operating conditions in terms of bias currents and peak-to-peak driving currents. The SIPM-OOFDM-DSPM signal BER versus DML bias current performances for various peak-to-peak driving currents are presented in Fig. 6 for the optical back-to-back (BTB) case. In numerically simulating Fig. 6, the received optical power is fixed at −13 dBm and the optical launch power is set at 5 dBm. It is observed in Fig. 6 that, for a fixed peak-to-peak driving current, over a bias current range of <20 mA, a reduction in bias current increases the BER mainly because of the low bias current-induced driving signal clipping effect. On the other hand, over a bias current range of >20 mA, the BERs increase slowly with increasing bias current. This is because of the high bias current-induced reduction in effective optical-to-signal power ratio (OSNR). Thus an optimum bias current occurs, which is almost
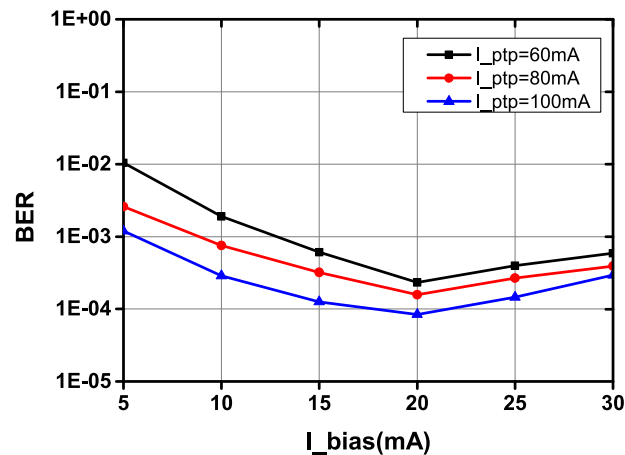
Fig. 6. BER versus bias current of directly modulated DFB laser with various peak-to-peak SIPM-OFDM-DSPM driving currents over optical back-to-back channels.
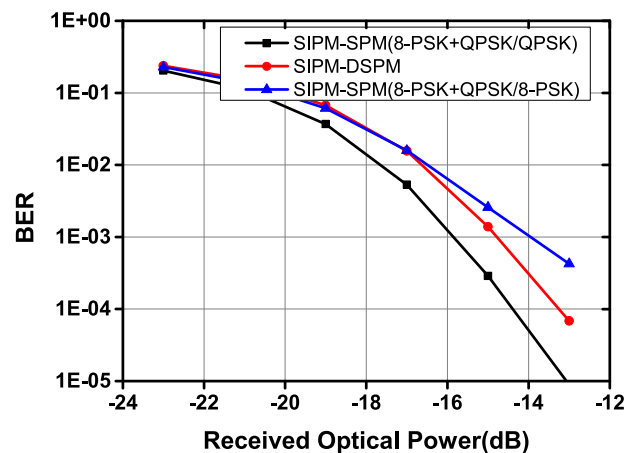

Fig. 7. BER versus received optical power over 25 km SSMF DML-based IMDD PON systems.

independent of the peak-to-peak driving current. At the optimum bias current, the BER decreases with increasing the peak-to-peak driving current, as presented in Fig. 6. This is mainly due to enhanced OSNRs associated with the large peak-to-peak driving currents. From the above analysis, a 20 mA bias current and a 100 mA peak-to-peak driving current can be regarded as the optimum DML operating conditions for the cases considered here.

For the 25 km SSMF IMDD PON systems incorporating the DML operating at the identified optimum operating conditions, the BER versus received optical power performances of the considered three transmission techniques are plotted in Fig. 7, where the optical launch powers are still fixed at 5 dBm. By comparing the BER performances between SIPM-OOFDM-DSPM, (8-PSK + QPSK)/QPSK-encoded SIPM-OOFDM-SPM and (8-PSK + QPSK)/8-PSK-encoded SIPM-OOFDM-SPM, it can be seen in Fig. 7 that a 1 dB received optical power penalty and a 0.9 dB power gain occurs respectively at a BER of 1.0×10^{-3}. This agrees very well with the characteristics observed in Fig. 4(a) and Fig. 5(a). In addition, compared to the optical BTB case, the 29.67 Gb/s SIPM-OOFDM-DSPM signal transmission over 25 km SSMF IMDD PON system suffers a 2 dB optical power penalty because of the DML-induced positive transient frequency chirp effect [15].

5. Conclusion

As an improved variant of the previously reported SIPM-OOFDM-SPM technique, SIPM-OOFDM-DSPM has been proposed and numerically explored, for the first time, in AWGN and DML-based IMDD PON systems. Based on the identified optimum key transceiver design parameters, the SIPM-OOFDM-DSPM transmission characteristics over various IMDD PON systems have been investigated. It is shown that SIPM-OOFDM-DSPM supports 29.67 Gb/s signal transmission over 25 km SSMF IMDD PON systems, which is an 11.1% increase in signal transmission capacity compared to the (8-PSK + QPSK)/QPSK-encoded SIPM-OOFDM-SPM technique. Compared to the (8-PSK + QPSK)/8-PSK-encoded SIPM-OOFDM-SPM technique delivering the same signal bit rate, the proposed technique considerably enhances the system power budget and performance tolerance to both chromatic dispersion and fiber nonlinearity. In addition, optimum DML operation conditions in terms of bias current and peak-to-peak driving current have also been identified. Compared to ideal optical intensity modulator cases, very similar SIPM-OOFDM-DSPM performance characteristics still remain in DML-based IMDD PON systems. The research suggests that SIPM-OOFDM-DSPM is a promising signal transmission technique capable of providing cost-sensitive IMDD PON systems with improved performance flexibility and adaptability.

References

[1] C.-X. Wang *et al.*, "Cellular architecture and key technologies for 5G wireless communication networks," *IEEE Commun. Mag.*, vol. 52, no. 2, pp. 122–130, Feb. 2014.
[2] V. Jungnickel *et al.*, "The role of small cells, coordinated multipoint, and massive MIMO in 5G," *IEEE Commun. Mag.*, vol. 52, no. 5, pp. 44–51, May 2014.
[3] S. Timotheou and I. Krikidis, "Fairness for non-orthogonal multiple access in 5G systems," *IEEE Signal Process. Lett.*, vol. 22, no. 10, pp. 1647–1651, Oct. 2015.
[4] Z. E. Ankarali, B. Pekoz, and H. Arslan, "Flexible radio access beyond 5G: A future projection on waveform, numerology, and frame design principles," *IEEE Access*, vol. 5, pp. 18295–18309, May 2017.
[5] R. Abu-Alhiga and H. Haas, "Subcarrier-index modulation OFDM," in *Proc. Int. Sym. IEEE Pers., Indoor Mobile Radio Commun.*, Sep. 2009, pp. 177–181.
[6] E. Başar, Ü. Aygölü, E. Panayırcı, and H. V. Poor, "Orthogonal frequency division multiplexing with index modulation," *IEEE Trans. Signal Process.*, vol. 61, no. 22, pp. 5536–5549, Nov. 2013.
[7] R. Fan, Y. J. Yu, and Y. L. Guan, "Generalization of orthogonal frequency division multiplexing with index modulation," *IEEE Trans. Wireless Commun.*, vol. 14, no. 10, pp. 5250–5359, Oct. 2015.
[8] E. Başar, "Index modulation techniques for 5G wireless networks," *IEEE Commun. Mag.*, vol. 54, no. 7, pp. 168–175, Jul. 2016.
[9] F. Halabi *et al.*, "Subcarrier index-power modulated optical OFDM(SIPM-OOFDM) for IMDD PON systems," in *Proc. Int. Conf. Opt. Fibre Commun.*, Mar. 2016, Paper Th3C.1.
[10] F. Halabi *et al.*, "Subcarrier index-power modulated optical OFDM and its performance in IMDD PON systems," *J. Lightw. Technol.*, vol. 34, no. 9, pp. 2228–2234, May 2016.
[11] L. Chen, F. Halabi, R. P. Giddings, and J. M. Tang, "Subcarrier index-power modulated optical OFDM with superposition multiplexing for IMDD transmission systems," *J. Lightw. Technol.*, vol. 34, no. 9, pp. 2228–2234, Oct. 2016.
[12] G. P. Agrawal, *Fibre-Optic Communication Systems*, 2nd ed. Hoboken, NJ, USA: Wiley, 1997.
[13] J. L. Wei, X. Q. Jin, and J. M. Tang, "The influence of directly modulated DFB lasers on the transmission performance of carrier suppressed single sideband optical OFDM signals over IMDD SMF systems," *J. Lightw. Technol.*, vol. 27, no. 13, pp. 2412–2419, Jul. 2009.
[14] J. E. A. Whiteaway, G. H. B. Thompson, A. J. Collar, and C. J. Armistead, "The design and assessment of λ/4 phase-shifted DFB laser structures," *IEEE J. Quantum Electron.*, vol. 25, no. 6, pp. 1261–1279, Jun. 1989.
[15] J. L. Wei, C. Sanchez, R. P. Giddings, E. Hugues-Salas, and J. M. Tang, "Significant improvements in optical power budgets of real-time optical OFDM PON systems," *Opt. Exp.*, vol. 29, no. 18, pp. 2861–2870, Sep. 2011.